Appl Phys A (2011) 103: 749–753
DOI 10.1007/s00339-010-6213-z

Applied Physics A
Materials Science & Processing

Enhanced broadband optical transmission in metallized woodpiles

R. Malureanu · A. Alabastri · W. Cheng · R. Kiyan · B. Chichkov · A. Andryieuski · A. Lavrinenko

Received: 14 January 2010 / Accepted: 3 December 2010 / Published online: 29 December 2010

Abstract We present an optimized isotropic metal deposition technique used for covering three-dimensional polymer structures with a 50 nm smooth silver layer. The technology allows fast and isotropic coating of complex 3D dielectric structures with thin silver layers. Transmission measurements of 3D metallized woodpiles reveal a new phenomenon of enhanced optical transmission in broadband range (up to 300 nm) in the near IR.

1 Introduction

Deposition of thin, smooth metal layers on three-dimensional structures is one of the challenges within thin film deposition field. Such structures have been proved to be extremely useful in a number of research fields and applications ranging from Raman spectroscopy [1] to metamaterials [2, 3], and from electronics [4] to medicine [5].

In this work we concentrate on the metal deposition aiming the three-dimensional (3D) metamaterials fabrication. After the first successes [6], the metamaterials research field has gained a huge momentum due to advances in theory, modeling and fabrication. One natural trend is toward increasing the operating frequency from microwaves to the IR and visible regime [7–9]. However, such tendency also brought challenges in the fabrication procedures due to the decrease in unit cell sizes and enhanced claims for needed resolution and accuracy.

Another trend in this field is to expand designs to truly 3D ones that can give bulk and eventually isotropic response within the frequency range of interest. In order to reach this target, several fabrication technologies have been developed. Among those, a layer by layer approach for fabrication of 3D metamaterials in IR has been demonstrated recently [9].

An alternative approach is to fabricate a 3D polymer skeleton structure with further metallization of its surface. The two-photon polymerization technique (2PP) [10] is proven to be very flexible and efficient technology for fabrication of 3D polymer layouts including structures for photonic applications [11]. Still, in spite of that several 3D metamaterials designs have been proposed [12, 13], their fabrication is severely hampered by the difficulty of controlled metal deposition on 3D structures with complex topology.

To the best of our knowledge, the two main methods for covering a polymer structure with metals are the chemical vapor deposition (CVD) and the "electroless" one. While the CVD method shows great promise in this respect [14], the parameter space is large thus the optimizing procedure claims exhaustive efforts due to the existence of multiple local minima. The electroless deposition technique provides much more reduced parameter space, thus easier optimization, and the lack of volatile poisonous products in the deposition process. Such technique was used in various recipes and with very good results in the photonics field also [15–18].

By metallization of polymer structures, new characteristics are observed within the transmission spectra. In the case of woodpiles, previous work [16] show the increase of the bandgap region as well as its strength. On the other hand, the

R. Malureanu (✉) · A. Alabastri · A. Andryieuski · A. Lavrinenko
DTU Fotonik, Technical University of Denmark, Copenhagen, Denmark
e-mail: rmal@fotonik.dtu.dk

A. Alabastri
Dipartimento di Fisica, Politecnico di Milano, Milan, Italy

W. Cheng · R. Kiyan · B. Chichkov
Laser Zentrum Hannover, Hannover, Germany

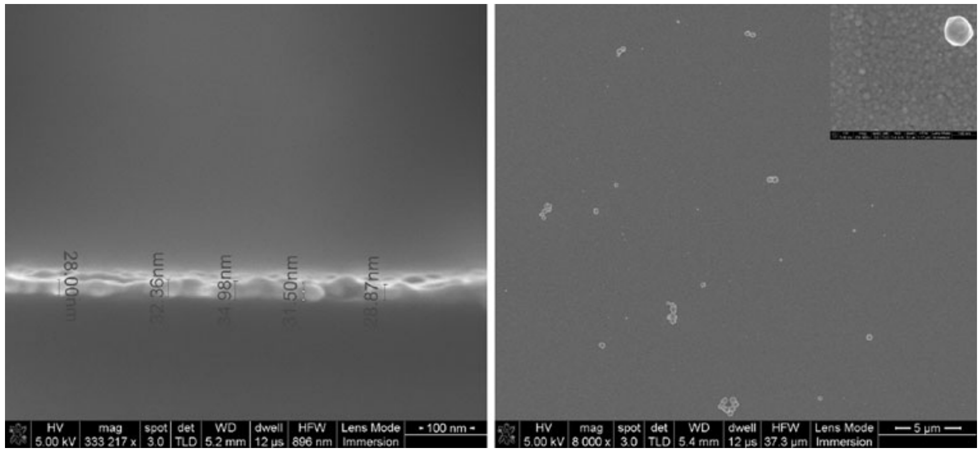

Fig. 1 (**a**) Ultrathin uniform silver layer deposited by the electroless technique on the silica substrate. Numbers show the thickness of the silver coating. (**b**) Top view of the sample showing high deposition uniformity over a large area. Some single Ag nanocrystals deposited on top of the layer are visible. In the inset, a zoom-in of the surface is shown

transmission characteristics at the edge of such structures are not extensively studied nor completely understood. In this work we show the existence of an enhanced broadband transmission region at such borders. This effect is present while measuring different randomly chosen structures thus eliminating the possibility of a measuring artifact.

2 Fabrication

Aiming for the potential applications of devices in the optical range, we decided to deposit thin and smooth metallic layers by optimizing the recipe known as Tollen's test or the silver mirror reaction [19, 20].

For our experiments we prepared stock solutions of silver nitrate 0.2 M and formaldehyde 8%. To get the silver ammonia complex, we mixed the stock silver nitrate solution with 27% ammonia water. The proportion was calculated such that all the silver nitrate is transformed into its ammonia complex but, at the same time, not to have extra-ammonia in solution. This way, the volumetric ratio silver nitrate:ammonia water has to be 21:1. The obtained solution was diluted 1:16 in MilliQ water. The reduction of silver complex to silver was performed by adding the diluted formaldehyde in a 1:80 volumetric ratio to the cooled silver ammonia solution. The deposition took place at low temperature (6°C). All the substances were obtained from Sigma-Aldrich.

Using the presented recipe, the thinnest complete layer obtained was of 30 nm thickness (Fig. 1a). Thinner silver layers are not completely formed, exhibiting random cluster formation. We think that this effect is due to the mechanism of the silver seed formation. In order to obtain a thinner layer, the initial silver seeds need to be both of high density and uniform size. By further optimization of the deposition parameters, such layer can be obtained.

In Fig. 1b we present a top-view showing high uniformity in the layer formation. The substrate is uniformly covered, but a few silver nanoparticles can be observed on top of its surface. These Ag nanocrystals are formed in solution and then they bind to the substrate in the ready form. Still, such nanocrystals formation is minimal and does not restrain the overall deposition process. In the inset of Fig. 1b one can see a zoom-in of the deposited layer where the polycrystalline growth of the silver is noticeable. Our samples were up to 1×1 cm in sizes, and no pronounced difference in layer properties was observed over such extended surface, thus showing the up-scaling possibilities of such technique.

The optimized deposited layer was measured using the atomic force microscopy technique. Before the deposition, the surface had 2 nm average roughness and 4 nm RMS while after the deposition the silver layer had 4 nm average roughness and 6 nm RMS thus having properties comparable with the ones of evaporated films.

After the optimization on a flat surface, we chose polymer woodpiles [21] for testing the deposition on complex 3D structures. This way we were able to check both the Ag deposition on the structure's sidewalls as well as inside the structure.

The samples were fabricated by two-photon polymerization processing of hybrid zirconium sol-gel photo-resist material [22]. Igacure 369 from Ciba was used as photoinitiator. The laser system consists of SHG Yb:Glass femtosecond laser with wavelength 513 nm, pulse duration 200 fs, and repetition rate 1 MHz. The photo-resist layer was deposited on the 150 µm thick glass slide. The laser beam was focused into the volume of the photo-resist through the glass slide by oil immersion $100\times$ microscope objective with numerical aperture of 1.4.

The fabricated woodpiles are 50×50 µm and have a height of about 16 µm corresponding to 8 periods (32 single layers) of the lattice. Sizes of the bars are 500×500 nm and they are periodically arranged with 2 µm period providing a face centered tetragonal lattice. We immersed the wafer into the depositing bath for 2 minutes thus obtaining an approximate 50 nm layer thickness. The results of silver de-

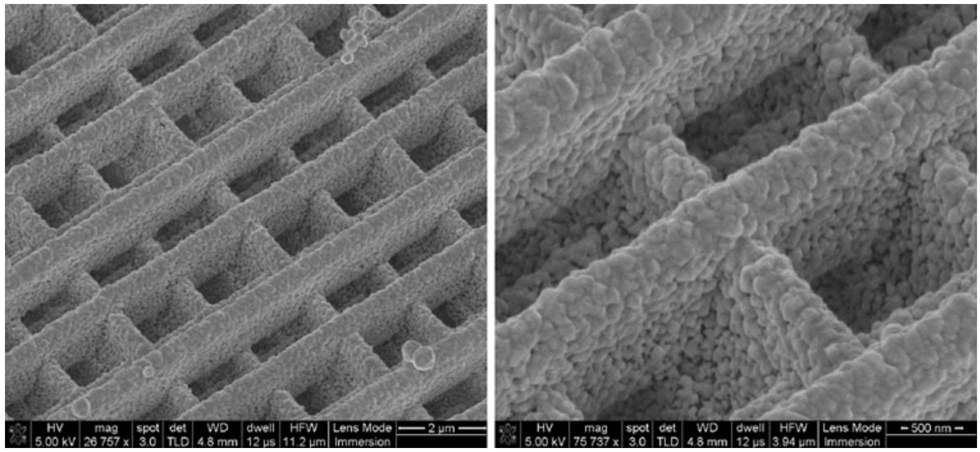

Fig. 2 (**a**) A 3D woodpile structure covered by silver after electroless deposition. Silver is deposited also all over the bulk structure and on structure's sidewalls. (**b**) Zoom-in of the 3D structure showing the deposition took place also inside the woodpile

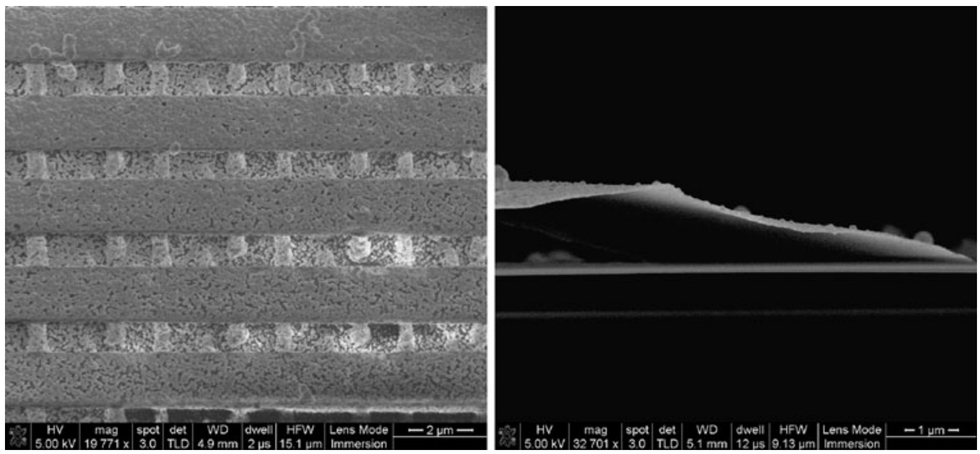

Fig. 3 (**a**) Sidewall SEM image of the woodpile. As can be seen, the deposition takes place all through the depth of the woodpile crystal. Here 5 periods in the vertical direction are presented. (**b**) An example of weak adhesion of the silver layer to the untreated silica surface. It illustrates the importance of pretreatment for a good adhesion

position are presented in Fig. 2a. The Ag layer is deposited not only on the top of the structure but also on its sidewalls. There is still particle formation in the solution followed by their adhesion to the deposited layer, but their influence on the transmission characteristics is minimal and can be neglected. A zoom-in of the 3D covered structure (Fig. 2b) shows the presence of silver layer inside the bulk structure as well.

We attribute the difference in layer quality deposited on the plane silica surface with respect to the one on the woodpile structure to the different chemical properties of the two samples surfaces.

One should note that the reaction is diffusion driven. Due to this aspect, the silver layer quality is monotonously decreasing from the top to the bottom of the structure (Fig. 3a). Nevertheless, the deposition took place everywhere covering the woodpile with a uniform silver coating. Further optimization of the recipe can lead to better in-depth coating of the structures.

An important aspect of the procedure is the pretreatment of the sample. The pretreatment solution was prepared by dissolving 2 g of $SnCl_2$ into 3 ml glacial acetic acid and 1 ml HCl and then diluting the obtained solution in a 1:100 volumetric proportion in MilliQ water. All the substances were obtained from Sigma-Aldrich. The samples are immersed for 10 min in the solution and then thoroughly rinsed in running water. As can be seen from Fig. 3b in the absence of the pretreatment, the silver layer is not adhering to the silica. In the same time this non-adhesion shows that, if needed, the silver can be selectively deposited on a structure by deliberate pretreatment of the surface. The obtained results are easily reproduced on various samples of different dimensions as long as the deposition conditions are the same.

3 Optical characterization

In order to characterize the structures, we used a fiber-based optical setup similar to the one described in [23]. The signal from a broadband source is transmitted through a polarizer and a polarization maintaining fiber to the sample. The transmitted signal is collected by another fiber and sent into an optical spectrum analyzer. Using such a setup, we are able to maintain the spot size below 10 µm; thus a precise positioning of the spot size on the woodpile is possible.

The first measures were performed on the non-covered woodpile structures. We tested transmission of several

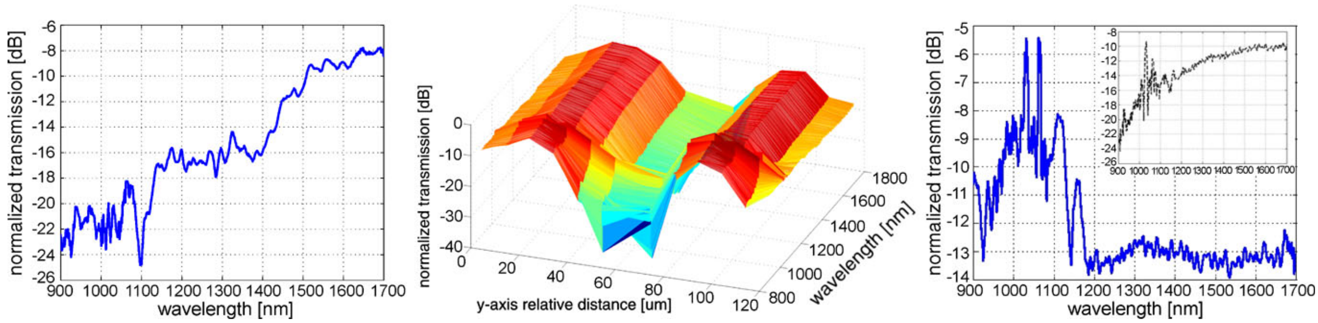

Fig. 4 (**a**) The obtained transmission spectra of a polymer woodpile. The two dips at 1100 and 1400 nm are identified as Bragg reflection peaks of the woodpile structure. (**b**) The spectra obtained while scanning the metallized sample along the y-axis. The two symmetrical transmission peaks are clearly visible at structure's edges ($y = 20$ nm and 90 nm). (**c**) The spectrum at the border of silver-covered woodpile structure. As can be seen, a wide transmission peak centers at 1050 nm is present and overimposed on several other narrow ones. In the inset, the transmission spectra outside the woodpile structure can be seen

woodpiles located in different parts of the wafer. The typical spectrum (Fig. 4a) shows transmission dips around 1100 nm and 1400 nm, which are repeatedly appearing in transmission through randomly chosen woodpile crystals. Considering that the polymer has no significant spectral signatures in this frequency range and the substrate is simple glass, the observed dips have to come from the geometry of the sample. Accordingly to simulations of such polymer woodpile performed with the periodical boundary conditions, transmission dips appear around 1000 nm and 1450 nm. Taking into account fabrications imperfections we get good corresponding in dips spectral positions. Therefore, we interpret observed dips as high-order Bragg reflection peaks occurring in a polymer woodpile structure acting as a 3D photonic crystal [24].

After coating with metal, the signal level in the central part of the structure dropped to the noise level. This decrement of transmission was anticipated due to the substantial number of the woodpile periods completely covered with silver. Meanwhile it confirms implicitly the complete silver deposition inside the bulk woodpile.

In order to obtain a measurable signal, we scanned the sample from one side to the other, measuring the transmission signal through the woodpile. In this configuration, the transmitted signal is increasing while moving from the center ($y = 60$ μm) to the borders of the structure ($y =$ 20 μm and 90 μm) and then decreasing rapidly when moving away from the structure (Fig. 4b). Such behavior is due to the deposition characteristics. Since the reaction is diffusion driven, the sample has a depleted region at the interface between the woodpile and the substrate. Owing to this depleted region, the transmission increases at the woodpile's border, thus explaining the 2-wing transmission dependence.

However, spectral behavior of transmission at the boundaries of a woodpile sample exhibits a remarkable feature. A typical transmission spectrum on the border of the structure is represented in Fig. 4c. There is a broad peak in the 900–1200 nm range with a pronounced level of transmitted signal, which cannot be assigned to the metallized photonic crystal behavior. We attribute this peak to the coupling of light to surface plasmon polariton (SPP) modes existing on the sidewalls of the woodpiles. SPPs modes transmit energy to the bottom of the structure signal and couple back to the optical modes, so that the signal is detected by the collecting fiber. This pronounced feature of broad band with enhanced transmission is not endemic for one particular woodpile crystal, but is statistically supported by observation on eight woodpile structures chosen in different parts of the woodpile array.

4 Conclusion

One of the main bottlenecks in advancing the fabrication of metamaterials is due to the difficulty of realizing isotropic, cost effective 3D deposition of metals on a desired structure. By using a combination of electroless deposition and 2PP techniques we believe that a viable solution for fabricating 3D bulk metamaterials can be found. In this work we present an optimized method for depositing silver on silica and silica-like substrates.

Such technique is not limited to the metamaterials field but it can be used for other research areas as well, where depositing of metals are required. We think that the technique reported here bears a great potential in many aspects of metal deposition in nanophysics.

The characterization of the polymer woodpile structures was performed both topologically and optically. The optical characterization shows huge behavioral difference with respect to the uncoated polymer structure. Such behavior is probably due both to the decrease in transmission spectra and to the existence of propagating surface plasmon polaritons on the sidewalls of the structure. The broad enhanced transmission band on the boundaries of woodpiles is a phenomenon which can have interesting potential application. We are planning to perform a detailed study of this boundary effect by simulating finite metallized woodpile structures.

Acknowledgements The authors acknowledge A. Boltasseva for allowing the use of the optical characterization setup. R. Malureanu, A. Andryieuski, A. Lavrinenko acknowledge financial support from NIMbus project funded by the Danish Research Council for Technology and Production Science. W. Cheng, R. Kiyan, B. Chichkov acknowledge the financial support of the Cluster of Excellence QUEST.

References

1. A. Campion, P. Kambhampati, Surface-enhanced Raman scattering. Chem. Soc. Rev. **27**, 241–250 (1998)
2. V.M. Shalaev, Transforming light. Science **322**, 384–386 (2008)
3. D. Schurig, J.J. Mock, B.J. Justice, S.A. Cummer, J.B. Pendry, A.F. Starr, D.R. Smith, Metamaterial electromagnetic cloak at microwave frequencies. Science **341**, 977–980 (2006)
4. T. Scheibel, R. Parthasarathy, G. Sawicki, X.-M. Lin, H. Jaeger, S.L. Lindquist, Conducting nanowires built by controlled self-assembly of amyloid fibers and selective metal deposition. Proc. Natl. Acad. Sci. USA **100**, 4527–4532 (2003)
5. S. Lal, S.E. Clare, N.J. Halas, Nanoshell-enabled photothermal cancer therapy: impending clinical impact. Acc. Chem. Res. **41**, 1842–1851 (2008)
6. R.A. Shelby, D.R. Smith, S.C. Nemat-Nasser, S. Schultz, Microwave transmission through a two-dimensional, isotropic, left-handed metamaterial. Appl. Phys. Lett. **78**, 489–491 (2001)
7. C. Enkrich, M. Wegener, S. Linden, S. Burger, L. Zschiedrich, F. Schmidt, J.F. Zhou, Th. Koschny, C.M. Soukoulis, Magnetic metamaterials at telecommunication and visible frequencies. Phys. Rev. Lett. **95**, 203901 (2005)
8. J. Valentine, S. Zhang, T. Zentgraf, E. Ulin-Avila, D.A. Genov, G. Bartat, X. Zhang, Three-dimensional optical metamaterial with a negative refractive index. Nature **455**, 376–379 (2008)
9. N. Liu, H. Guo, L. Fu, S. Kaiser, H. Schweizer, H. Giessen, Three-dimensional photonic metamaterials at optical frequencies. Nat. Mater. **7**, 31–37 (2008)
10. S. Maruo, O. Nakamura, S. Kawata, Three-dimensional microfabrication with two-photon-absorbed photopolymerization. Opt. Lett. **22**, 132–134 (1997)
11. J. Serbin, A. Ovsianikov, B. Chichkov, Fabrication of woodpile structures by two-photon polymerization and investigation of their optical properties. Opt. Express **12**, 5221–5228 (2004)
12. A. Alú, N. Engheta, The quest for magnetic plasmons at optical frequencies. Opt. Express **17**, 5723–5730 (2009)
13. A. Andryieuski, R. Malureanu, A. Lavrinenko, Nested structures approach in designing an isotropic negative-index material for infrared. J. Eur. Opt. Soc., Rapid Publ. **4**, 09003 (2009)
14. M.S. Rill, C. Plet, M. Thiel, I. Staude, G. von Freymann, S. Linden, M. Wegener, Photonic metamaterials by direct laser writing and silver chemical vapour deposition. Nat. Mater. **7**, 543–546 (2008)
15. Y.S. Chen, A. Tal, D.B. Torrance, S.M. Kuebler, Fabrication and characterization of three-dimensional silver-coated polymeric microstructures. Adv. Funct. Mater. **16**, 1739–1744 (2006)
16. K. Kaneko, K. Yamamoto, S. Kawata, H. Xia, J.-F. Song, H.-B. Sun, Metal-nanoshelled three-dimensional photonic lattices. Opt. Lett. **33**, 1999–2001 (2008)
17. F. Formanek, N. Takeyasu, T. Tanaka, K. Chiyoda, A. Ishikawa, S. Kawata, Selective electroless plating to fabricate complex three-dimensional metallic micro/nanostructures. Appl. Phys. Lett. **88**, 083110 (2006)
18. N. Takeyasu, T. Tanaka, S. Kawata, Fabrication of 3D metal/polymer microstructures by site-selective metal coating. Appl. Phys. A **90**, 205–209 (2008)
19. R.W. Furness, *The Practice of Plating on Plastics* (Teddington Press, Surrey, 1968)
20. S.Q. Wang, H. Zhao, Y. Wang, C.M. Li, Z.H. Chen, V. Paulose, Silver-coated near field optical scanning microscope probes fabricated by silver mirror reaction. Appl. Phys. B, Lasers Opt. **92**, 49–52 (2008)
21. S.Y. Lin, J.G. Fleming, D.L. Hetherington, B.K. Smith, R. Biswas, K.M. Ho, M.M. Sigalas, W. Zubrzycki, S.R. Kurts, J. Bur, A three-dimensional photonic crystal operating at infrared wavelengths. Nature **394**, 251–253 (1998)
22. A. Ovsianikov, J. Viertl, B. Chichkov, M. Oubaha, B. MacCraith, I. Sakellari, A. Giakoumaki, D. Gray, M. Vamvakaki, M. Fasari, C. Fotakis, Ultra-low shrinkage hybrid photosensitive material for two-photon polymerization microfabrication. ACS Nano **2**, 2257–2262 (2008)
23. A. Boltasseva, S.I. Bozhevolnyi, T. Nikolajsen, K. Leosson, Compact Bragg gratings for long-range surface plasmon polaritons. J. Lightwave Technol. **24**, 912–918 (2006)
24. M. Deubel, M. Wegener, S. Linden, G. von Freymann, Angle-resolved transmission spectroscopy of three-dimensional photonic crystals fabricated by direct laser writing. Appl. Phys. Lett. **87**, 221104 (2005)